Dynamically reconfigurable liquid-core liquid-cladding lens in a microfluidic channel†

Sindy K. Y. Tang, Claudiu A. Stan and George M. Whitesides*

Received 5th November 2007, Accepted 14th December 2007
First published as an Advance Article on the web 14th January 2008
DOI: 10.1039/b717037h

This paper describes the design and operation of a liquid-core liquid-cladding (L^2) lens formed by the laminar flow of three streams of liquids in a microchannel whose width expands laterally in the region where the lens forms. Two streams of liquid with a lower refractive index (the cladding) sandwich a stream of liquid with a higher refractive index (the core). As the core stream enters the expansion chamber, it widens and becomes biconvex in shape, for some rates of flow. This biconvex fluidic element focuses light. Manipulating the relative rates of flow of the streams reconfigures the shape, and therefore the focal distance, of the L^2 lens. This paper also describes a technique for beam tracing, and for characterization of a lens in an enclosed micro-scale optical system. The use of a cladding liquid with refractive index matched to that of the material used in the fabrication of the microfluidic system (here, poly(dimethylsiloxane)) improves the quality of the focused beam.

Introduction

This paper describes the design and operation of a dynamically reconfigurable microfluidic lens for use in microfluidic systems; this lens focuses light originating in the plane of a planar array of microfluidic channels in that same plane. The lens is formed by laminar flow of three streams of fluids; the index of refraction of the central ("core") stream is higher than the index of the sandwiching ("cladding") streams. The streams enter a microchannel having a region in which the channel expands laterally. Fig. 1a shows this system schematically: the central portion of the channel responsible for lensing (the "expansion chamber") is ten times wider than the entrance and exit. In the inlet and outlet channels, the interface between the core and the cladding streams is straight and parallel to the channel. In the expansion chamber, the width of the core stream increases and then decreases. For some rates of flow, the shape of the interface between the core and cladding streams in the expansion chamber is biconvex.

We use this fluidic biconvex structure as a lens to focus light propagating in the plane of the expansion chamber, and perpendicular to the direction of flow of the fluids. By changing the relative rates of flow of the three streams, we change the curvature of the interface and thus the focal distance of the lens in real time. Since the optical interface is formed between a liquid-core and a liquid-cladding, we refer to this lens as an L^2 lens.

Focusing of light in a microfluidic device is important for lab-on-a-chip applications that require optical characterization. Efficient illumination and collection of light from limited areas of the microchannel can be critical in the performance of the device. An example is a microfluidic flow cytometer, where localized excitation of fluorescent labels in cells or beads is essential in counting them accurately.[1,2] It is difficult, however, to use conventional free-space optical components to couple and focus light into the plane of a microfluidic device. A common way of introducing light into the device is through the insertion of optical fibers. Optical fibers facilitate optical alignment between external light sources, or detectors, and the microfluidic channel, and allow more flexibility in system design.

Light from an optical fiber is diverging, however, and requires collimation and focusing. Several groups have fabricated planar lens-shaped features for focusing light in microfluidic systems.[3–6] The quality of these lenses depends on the smoothness of the side wall of the channels, and the focal length of the lenses is usually fixed. Most tunable lenses reported can only focus light perpendicular to the plane of the device.[7–15] Our lens based on the laminar flow of multiple streams of fluids focuses light in the plane of the microchannels, and possesses the following attractive characteristics: (i) the lens is dynamically reconfigurable—the rates of flow of the fluids change the curvature and the focal distance of the lens in real time. The choice of fluids determines the contrast in refractive indices across the core and cladding streams, and the wall of the channel. (ii) Since the device operates in the low Reynolds number regime, the flow is laminar (that is, occurs without turbulent mixing).[16] The interface between the core and the cladding streams is optically smooth despite the roughness on the wall of the channel.[17] It is thus possible to use low-precision fabrication to make the microfluidic channels, and still produce high-quality optical interfaces. By using a cladding liquid with refractive index matched to that of PDMS, it is possible to reduce losses due to scattering of light on the side wall of the microchannel. (iii) Since the L^2 lens is formed inside a microfluidic channel

Department of Chemistry and Chemical Biology, Harvard University, 12 Oxford St., Cambridge, MA 02138, USA.
E-mail: gwhitesides@gmwgroup.harvard.edu

† Electronic supplementary information (ESI) available: Fig. S1–S5 and Table S1. See DOI: 10.1039/b717037h

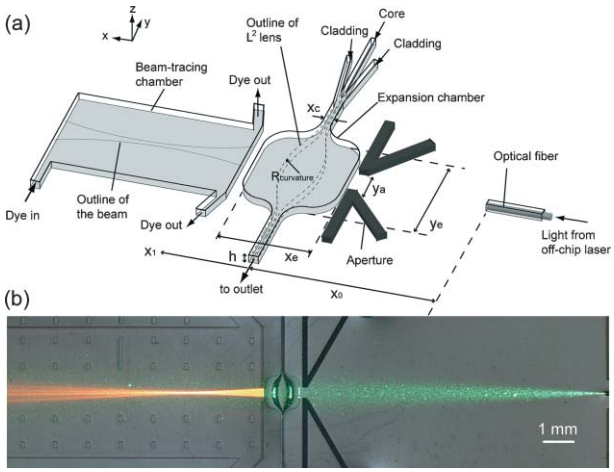

Fig. 1 (a) Schematic representation of the experimental setup for focusing light exiting an optical fiber through the liquid-core liquid-cladding (L^2) lens. The distance between the light source and the center of the lens, x_0, is 10 mm. The aperture is formed by two channels filled with black ink after fabrication. The size of the aperture, y_a, is 334 μm. The channel for the formation of the L^2 lens contains a square expansion chamber. The solid lines show the walls of the channel, and the dashed lines show the interfaces between the core and the cladding streams. $R_{curvature}$ is the radius of curvature of this interface. The width of the channel at the inlet and outlet, x_c, is 100 μm. The width, x_e, and length, y_e, of the expansion chamber are both 1 mm. The radius of curvature of the rounded corners is 250 μm. The height (h) of the channel is about 100 μm. The beam-tracing chamber behind the L^2 lens is filled with solution of a fluorescent dye (2.5 μm Rhodamine 640 perchlorate in ethylene glycol) to make the optical path visible. (b) Bright-field image of the L^2 lens in operation taken using a CCD camera mounted on a Nikon AZ100 microscope with a 0.5× objective. In the figure, the core stream is benzothiazole, and the cladding stream is trifluoroethanol. The flow rate of the core was at 3 mL h^{-1}, and the flow rate of the claddings was at 7 mL h^{-1}. The green laser beam from the fiber is visible in front of the aperture because PDMS contains nanoparticles of silica that scatter light. The focused beam in the beam-tracing chamber is orange due to the fluorescence of the dye. The shadow at the core-cladding interface is partly due to the gradual change of the refractive index across the interface, and partly due to the density mismatch between the core and the cladding liquids (see text).

using co-fabrication (the design and fabrication of all functional components in a single step of microfabrication), integration and pre-alignment of the lens and other microfluidic components is simple.

Experimental design and operation

Fabrication of the device

We fabricated the microfluidic channels in PDMS using soft lithography.[18] PDMS is transparent in the visible wavelengths. It is therefore possible to enclose optical components in PDMS, and couple light through PDMS, with minimal loss due to absorption.[19]

Design of the microchannel for the formation of L^2 lens

To form the L^2 lens, we used a microchannel with a lateral expansion: the expansion chamber (width x_e = 1 mm, length y_e = 1 mm) was ten times wider than the inlet and outlet (width x_c = 100 μm) (Fig. 1a). This expansion ratio (x_e : x_c) allowed a sufficiently large variation in the curvature of the liquid core–liquid cladding interface to demonstrate the tunability of the focus of the lens. We chose a rectangular shape for the expansion chamber because a rectangular chamber does not cause light to converge or diverge when filled with a liquid with homogeneous refractive index. It allowed us to study the focusing effect of the L^2 lens as a function only of the curvature of the core–cladding interface. The one-to-one aspect ratio (x_e : y_e = 1 : 1) allowed a tight curvature of the core–cladding interface while keeping the L^2 lens relatively thin in the x-direction.[20] The corners of the expansion chamber were rounded to avoid undesired asymmetry in the shape of the L^2 lens due to recirculation zones,[21–25] which were more prominent and asymmetrical in size in chambers with sharp corners (Fig. S1 in the ESI).† The height of the channel was about 100 μm to accommodate the optical fiber (outer diameter ~ 100 μm) inserted into the device as the source of light.

The choice of liquids

We allowed three streams of liquids—a core stream sandwiched by two cladding streams—to flow laminarly in the microfluidic channel to form the L^2 lens. To achieve short focal distance for lab-on-a-chip applications, we explored liquids with high contrast in refractive indices. In principle, any liquids that do not swell PDMS[26] can be used to form the lens. As long as the contrast in refractive indices is large enough ($\Delta n_D > \sim 0.1$), the focal point of the lens should lie within the PDMS device (~2 cm × 2 cm).[27] We have used benzyl alcohol ($n_D^{22} = 1.540$, density $\rho = 1.04$ g cm^{-3}), and benzothiazole ($n_D^{22} = 1.641$, $\rho = 1.24$ g cm^{-3}) as the core liquid. Among common liquids with high refractive index[28] ($n_D > 1.5$), benzyl alcohol and benzothiazole[29] are relatively non-toxic and have relatively high values of n_D. Table S1 in the ESI† contains a list of refractive indices and hazard codes for selected liquids.

For the cladding liquid, we have used trifluoroethanol ($n_D^{22} = 1.291$, $\rho = 1.37$ g cm^{-3}), methanol ($n_D^{22} = 1.327$, $\rho = 0.79$ g cm^{-3}), a mixture of 73.5% ethylene glycol ($n_D^{22} = 1.429$, $\rho = 1.11$ g cm^{-3}) and 26.5% ethanol (n_D^{22} = 1.360, ρ = 0.79 g cm^{-3}) with the effective refractive index matched to that of PDMS (n_D^{22} = 1.412). We have also used a mixture of 53.6% trifluoroethanol, 31.5% benzothiazole and 14.9% ethanol with effective refractive index matched to that of PDMS, and effective density matched to that of benzothiazole ($\rho = 1.24$ g cm^{-3}). These cladding liquids are miscible with both benzyl alcohol and benzothiazole.

We were able to focus light using any combination of these core-cladding liquids. To demonstrate the principle of the L^2 lens, we focused on benzothiazole as the core, and the mixture of ethylene glycol and ethanol as the cladding for most of our experiments because: (i) they possess a sufficiently large contrast in refractive indices to allow the observation of the focus of the L^2 lens on the PDMS device at various curvatures of the core-cladding interface; (ii) matching the effective refractive index of the cladding to that of PDMS reduces loss due to scattering of light on the side wall of the microchannel, and improves the quality of the focused beam. For the experiments to evaluate the efficiency and light enhancement of the lens, we used benzothiazole as the core, and the mixture of trifluoroethanol,

benzothiazole and ethanol as the cladding because matching the density between the core and the cladding liquids was important in improving the quality of the core–cladding interface, and therefore the performance of the lens.

Experimental system used to characterize the L² lens

Fig. 1a shows the experimental system schematically, and Fig. 1b shows a photograph of the L² lens in operation. Light from a continuous-wave frequency-doubled Nd:YAG laser (532 nm, 95 mW) was coupled into the PDMS device using a single-mode optical fiber (nominal numerical aperture, $NA = 0.12$). We fixed the distance between the tip of the fiber and the center of the channel (x_0) to be 10 mm. This length scale allowed the focusing of light by the L² lens to occur on the same PDMS device, and facilitated observation using a microscope. The fiber was pointed toward the center of the lens. The optical path was perpendicular to the direction of flow of the fluids.

To facilitate beam tracing and determination of the focal point of the L² lens, we included an aperture in front of the expansion chamber to block incident light from regions of the lens close to the inlet and outlet where the radius of curvature is highly non-uniform (Fig. 1a). The size of the aperture was one-third of the size of the expansion chamber ($y_a = 334\ \mu m$) and was formed by two separate channels filled with black ink. For applications that require higher intensity at the focus, the aperture can be removed.

In order to visualize the optical path, we introduced fluorescent dyes (2.5 μM Rhodamine 640 perchlorate in ethylene glycol) in a chamber ("beam-tracing chamber") behind the L² lens. The solution of dye fluoresced only in regions where there was optical illumination. The concentration of the dye solution was sufficiently low such that the incident light could propagate through the beam-tracing chamber without being significantly attenuated or absorbed. The intensity of the incident light was sufficiently low to avoid photobleaching of the dye during the experiment.

Operation and data acquisition

To operate the L² lens, we pumped the core and cladding liquids contained in 10 mL-plastic syringes (Becton Dickinson 'Luer-Lok' series) at fixed volumetric flow rates using syringe pumps (Harvard Apparatus PHD 2000). To analyze the shape of the L² lens, the device was imaged on a charge-coupled device (CCD) camera using a Leica DMRX microscope with a 1.6× objective. To extract the focal distance of the lens, we recorded the fluorescence in the beam-tracing chamber using the same setup.

Results and discussions

Manipulating the shape of the L² lens

Fig. 2 shows the shapes of the L² lens under different flow conditions. The flow was quasi-two dimensional since the height of the expansion chamber was much smaller than its width and length. When the rates of flow of the left and the right cladding streams were the same, the core stream, or, the L² lens, was biconvex and symmetrical inside the expansion chamber. We

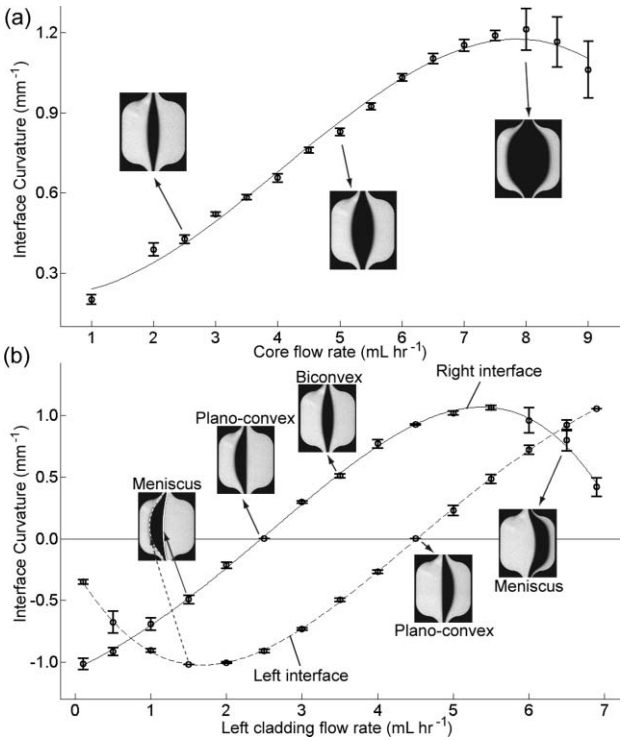

Fig. 2 (a) Curvature ($R^{-1}_{curvature}$) of the L² lens as a function of the rates of flow of the core stream. $R_{curvature}$ is the fitted radius of curvature of the core-cladding interface excluding regions where light was blocked by the aperture (see text). The core liquid was benzothiazole, and the cladding liquid was a mixture of ethylene glycol and ethanol with effective refractive index matched to that of PDMS. The flow rates for the left and right claddings were the same. The total flow rate of the core and both claddings was fixed constant at 10 mL h^{-1}. The insets show the fluorescence images of the L² lens in the expansion chamber at various flow rates. (b) Curvature of the left (dashed line) and right (solid line) interfaces of the lens as a function of the flow rate of the left cladding. The sign of curvature is positive (negative) if the center of curvature lies to the left (right) of the interface. The flow rate of the core was fixed at 3 mL h^{-1}. The sum of flow rates of the left and right claddings was fixed at 7 mL h^{-1}. The insets show the fluorescence images of the L² lens in the expansion chamber at the indicated flow rates. For both (a) and (b) the cladding liquid was dyed to make it easily imaged; the dye was omitted in normal operation of the L² lens. The data are the mean of three experimental runs. The error bars are the standard deviations of the curvatures measured at identical settings of rates of flow in different experimental runs. The lines are guides to the eye only.

extracted the radius of curvature ($R_{curvature}$) of the lens by fitting circles to the interface between the core and cladding streams in the recorded images of the L² lens. We excluded regions where light was blocked by the aperture. Fig. 2a shows the curvature ($R^{-1}_{curvature}$) of the left and right interfaces of this biconvex lens as a function of the rate of flow of the core stream (Q_{core}). We fixed the sum of the rates of flow of all streams at 10 mL h^{-1} (mean velocity in the expansion chamber $v_{mean} \sim 0.028$ m s^{-1}, Reynolds number $Re \sim 0.6$). This rate of flow was a compromise between the need to minimize diffusive broadening of the core-cladding interface (which decreases the contrast in refractive indices) by using a higher flow rate,[17,30–32] and the need to avoid asymmetrical flow when the total flow rate is much greater than 10 mL h^{-1} (Fig. S1 in ESI).†

As the flow rate of the core increased, the curvature first increased, and then decreased as the core-cladding interface approached the wall of the chamber. Increasing the ratio of viscosity between the core and cladding liquids had the same effect at fixed flow rates (results not reported here). The thickness of the lens (in the x-direction) also increased as the flow rate of the core increased. We do not report this variation here because the effect on the focal distance of the L^2 lens due to different thicknesses of the lens was insignificant, and was dominated by the curvature of the lens.[33]

We were able to achieve other shapes of the L^2 lens by varying the curvatures of the left and right interfaces separately. Fig. 2b shows the shapes of the lens obtained, and the curvatures of the left and right interfaces of the lens as a function of the rate of flow of the left cladding. We defined the sign of curvature to be positive (negative) if the center of curvature lies to the left (right) of the interface. We kept the flow of the core stream fixed at 3 mL h^{-1}. The thickness of the lens was, therefore, roughly constant. By varying the relative flow rate between the left and the right claddings, we were able to vary the curvatures of the left and right interfaces to obtain an extensive range of lens shapes: meniscus, plano-convex, and biconvex. Note that the curves for the left and right interfaces are basically the same; they are reflected about a left cladding flow rate of 3.5 mL h^{-1}, and also reflected about $R^{-1}_{\text{curvature}} = 0$.

Typically, the flow, or, the shape of the L^2 lens, stabilized in 30–60 seconds after we changed the volumetric flow rate on the syringe pump. We found that the type of syringes we used affected the response of the lens. Using a 1 mL-rigid syringe made of glass, the radius of curvature of the lens approached its new value with a relaxation time[34] of a few hundred milliseconds. With a softer 10 mL-plastic syringe, the relaxation time was on the order of ten seconds (Fig. S2 in ESI).† The plastic syringe, however, reduced fluctuations in the flow caused by the syringe pump significantly (Fig. S3 in ESI).† We used plastic syringes for most of our experiments, and we waited 180 seconds after we changed the flow rate before we recorded the data.

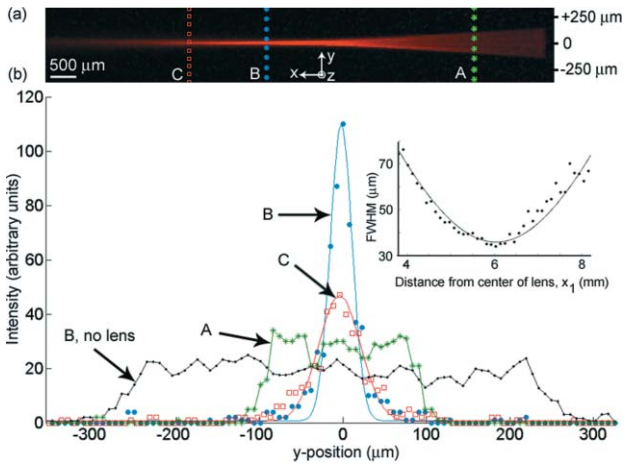

Fig. 3 (a) An optical micrograph of the focused beam recorded with a CCD camera mounted above the PDMS device through a Leica DMRX microscope with a 1.6× objective and a 600 nm long pass interference filter. Light propagated from the right side of the image to the left side of the image. The dashed lines with markers (*, ●, □) indicate the three positions (A, B, and C) at which the intensity profiles were plotted in (b). The original image file was in 8-bit format (256 gray levels). (b) Intensity profiles of fluorescence at locations (A, B and C) in the beam-tracing chamber, indicated by markers (*, ●, □) respectively. The lines are Gaussian curves fitted to the data. The inset shows the variation in beam width as a function of the distance from the center of the L^2 lens (x_1). The line is a hyperbola fitted to the data. The focal point is defined as the point with minimum beam width on the hyperbola. The core liquid was benzothiazole, and the cladding liquid was a mixture of 53.6% trifluoroethanol, 31.5% benzothiazole and 14.9% ethanol with effective refractive index matched to that of PDMS ($n_D^{22} = 1.412$), and density matched to that of benzothiazole in the core stream ($\rho = 1.24$ g cm^{-3}). The flow rates of the core and cladding streams were both at 5 mL h^{-1}. The intensity profile at position A was flat rather than Gaussian because the aperture blocked the edges of the incoming light beam. The FWHM of the fitted Gaussian curve, however, was still a good approximation of the width of the beam. We also plotted the intensity profile of the unfocused beam (no lens) at position B for comparison. The enhancement factor was about 4.6, and the efficiency of the lens was about 60% (see text for discussion).

The L^2 lens focuses light

Fig. 3a shows an optical micrograph of a focused beam at a core flow rate of 5 mL h^{-1} and a total cladding flow rate of 5 mL h^{-1}. Fig. 3b shows the variation in the intensity of fluorescence in the beam-tracing chamber at three different distances, indicated in Fig. 3a, from the L^2 lens. We fitted Gaussian curves[35] to the intensity profiles, and extracted the beam widths (defined as the full width at half maximum (FWHM) of the fitted Gaussian curve here) at different distances. The intensity profile at position A was flat rather than Gaussian because the aperture blocked the edges of the incoming light beam. The FWHM of the fitted Gaussian curve, however, was still a good approximation of the width of the beam. The inset in Fig. 3b shows the variation in the beam width and a fitted hyperbola[35] as a function of the distance from the center of the lens (x_1). We defined the point with the minimum beam width on the hyperbola as the focal point, and the distance between the focal point and the center of the L^2 lens as the focal distance.[36] At the focal point, the FWHM of the beam imaged with a 1.6× objective was 35 μm, close to the imaging setup's optical resolution, which we measured to be 28 μm using a resolution test target. To measure the beam width accurately, we used a microscope objective with 5× magnification, and a further 1.6× lens tube magnification. The resolution of this setup was 5.5 μm. We measured the FWHM of the beam at the focus to be approximately 16 μm, about 20 times less than the initial beam width (Fig. S4 in ESI).† This beam size was limited by aberration due to the shape of the L^2 lens; the diffraction-limited width at the focal point is approximately 7 μm using a 334 μm aperture.[37]

In addition to generating a narrow beam, the ability to enhance the intensity of light is also an important parameter for characterizing a lens for practical lab-on-a-chip applications. When reported, the enhancement factors (here defined as the ratio of the peak intensity of a focused beam to the intensity of an unfocused beam at the same point) were usually between 3 and 4 among previous work on on-chip cylindrical lenses.[4–6,38] The highest factor was 7 using compound microlenses for correction of aberration.[4] For the data in Fig. 3, this factor was 4.6, and it was 9 without any aperture (Fig. S5b in ESI).†

As far as we know, the enhancement factor of our L^2 lens is the highest among on-chip cylindrical lenses fabricated with standard planar lithographic procedures.

For the data in Fig. 3, in addition to matching the refractive index of the cladding liquid to that of PDMS, we also matched the density of the cladding liquid to that of the core liquid by using a mixture of 53.6% trifluoroethanol, 31.5% benzothiazole and 14.9% ethanol (effective $n_D^{22} = 1.412$; effective $\rho = 1.24$ g cm^{-3}) as the cladding. We found that matching the density between the core and the cladding liquids was important in achieving a higher enhancement factor. The L^2 lens formed by using the mixture of 73.5% ethylene glycol and 26.5% ethanol (effective $\rho = 1.03$ g cm^{-3}) as the cladding focused light in a similar way, but the enhancement factor was only about 2.5 (compared with 4.6 when using the density-matched cladding in the same device). We believe that the density mismatch between this mixture and benzothiazole caused the core-cladding interface to be slanted.[39–41] A slanted interface refracts the focused light out of the plane of the channels, and lowers the enhancement factor.

After matching the densities between the core and the cladding liquids, the efficiency of L^2 lens (defined here as the integrated light intensity of the focused beam relative to that of an unfocused beam) was about 60%. We are currently investigating the potential causes for the loss of light. We think that a non-uniform diffusion profile[32] between the core and cladding liquids led to a non-uniform refractive index profile at the core-cladding interface. This profile could cause an undesired refraction of light out of the plane of propagation. It should be possible to reduce this loss by incorporating the channel in a planar waveguide, for example, by forming the side walls of the channel with a material possessing a higher refractive index than the top and bottom walls.[5] The use of immiscible liquids in the core and the cladding streams can eliminate diffusion completely. Different wetting properties of the liquids on the PDMS wall and surface tension between the liquids (leading to droplet formation), however, complicated the flow and made the manipulation of the L^2 lens more difficult.

We have not calibrated the pixel intensity values recorded by the CCD camera (0 is the darkest level, and 255 is the brightest level) against the actual light intensity. The beam-tracing chamber, however, should still offer a reliable method to monitor the width of the focused beam as it propagates. As long as the camera is not saturated (that is, the maximum pixel intensity of the image is below 255), and the recorded signal is linear with respect to the incident light intensity, the Gaussian width of the beam is independent of its amplitude, and should not depend on the camera settings (such as exposure and integration time) and lighting conditions. Under these conditions, the intensity of the focused beam relative to the unfocused beam should also be a valid measurement of the enhancement factor of the lens. The data for extracting the FWHM of the focused beam and the enhancement factors were recorded in the linear regime of the camera.

The focal distance of the L^2 lens is tunable

To demonstrate the tunability of the focal distance of the L^2 lens in real time, we focused on the biconvex lens where the flow rates of the left and right claddings were equal. Fig. 4 shows the focal distance, measured from the center of the lens to the focal point, as a function of the core flow rate.[42] The core liquid was benzothiazole, and the cladding liquid was the mixture of ethylene glycol and ethanol with refractive index matched to that of PDMS. The variation of the focal distance follows the variation of the curvature of the lens (Fig. 2a) as expected from geometrical optics: a lens with a higher curvature focuses light at a shorter distance than one with a lower curvature. It is possible to achieve even shorter focal distances by using a cladding liquid with lower refractive index. The use of a smaller expansion chamber at the same expansion ratio reduces the radius of curvature of the core-cladding interface; the resulting focal distance should also be shorter.

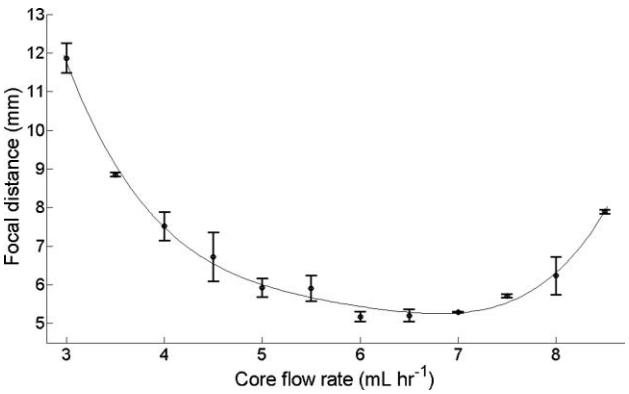

Fig. 4 Focal distance of the L^2 lens as a function of the rate of flow of the core stream. The core liquid was benzothiazole, and the cladding liquid was a mixture of ethylene glycol and ethanol with effective refractive index matched to that of PDMS. The total rate of flow of the core and cladding streams was fixed at 10 mL h^{-1}. The line is a guide to the eye only. The lenses formed at $Q_{core} = 2$ mL h^{-1} and $Q_{core} = 9$ mL h^{-1} also focused light. The focal distances were longer than the beam-tracing chamber, however, and we have not reported those data. The data are the mean of three experimental runs. The error bars are the standard deviations of the focal distances measured at identical settings of rates of flow in different experimental runs. Since the beam-tracing chamber was filled with a dye dissolved in ethylene glycol ($n_D^{22} = 1.429$), the measured focal distance here was longer than the case when the beam propagated in PDMS ($n_D^{22} = 1.412$) only. See text for discussions.

Quality of the lens

Fig. 5a and b compare the quality of the focused beam under the same flow conditions using a 500 μm-aperture and a 334 μm-aperture respectively. Although the intensity of the focused beam was higher in the former case, the aberration of the L^2 lens was more prominent: the areas of high light intensity were not limited to the paraxial focal point. This aberration is caused by the deviation of the shape of the core–cladding interface from the ideal lens shape. It was difficult to determine the paraxial focal point correctly when there was more aberration (also see Fig. S5a in ESI).† We therefore included the 334 μm-aperture for most of our experiments to facilitate the characterization of the L^2 lens. It should be possible to correct for the aberration by making small adjustments to the shape of the expansion chamber and fine-tuning the shape of the lens. We have not demonstrated this capability in the current work.

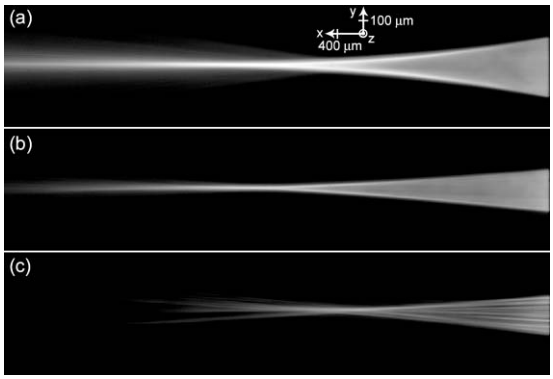

Fig. 5 Optical micrographs of the focused beam using (a) a 500 μm-aperture, and (b) a 334 μm-aperture, respectively. The core liquid was benzothiazole and the cladding liquid was a mixture of ethylene glycol and ethanol with effective refractive index matched to that of PDMS. The core flow rate was 6 mL h^{-1}, and the cladding flow rate was 4 mL h^{-1}. Aberration was more prominent in (a) using a 500 μm-aperture. (c) Optical micrograph of the focused beam using trifluoroethanol as the cladding liquid. The core liquid was benzothiazole. The aperture size was 334 μm. The core flow rate was 3 mL h^{-1}, and the cladding flow rate was 7 mL h^{-1}. Compared with (a) and (b), beam quality decreased due to the scattering of light at the PDMS-cladding interface. The beam-tracing chamber was filled with Rhodamine 640 perchlorate in a mixture of ethylene glycol and ethanol with index matched to PDMS for all cases above.

Fig. 5c shows the image of the focused beam using a L^2 lens with trifluoroethanol ($n_D^{22} = 1.291$) as the cladding liquid and benzothiazole as the core liquid. The focal distance achieved in this case was smaller due to the higher contrast in refractive indices between the core and the cladding. The quality of the beam was, however, visibly worse than the case when the index of the cladding liquid was matched to that of PDMS. The streaks in the light beam were due to scattering of light from the rough channel wall.

Conclusion

As our work approached completion, we learnt about the development of another hydrodynamically tunable cylindrical lens, based on centrifugal effect on a pair of density-mismatched liquids.[38] This lens has less light collection area, a smaller enhancement in intensity (the enhancement factor was about 1.6), and a smaller tuning range than our L^2 lens. It focuses light perpendicular to the plane of the microfluidic channels (in the *x*-*z* plane) while ours focuses light along the plane of the channels (in the *x*-*y* plane). The combination of this lens and our L^2 lens could, however, be potentially useful for three-dimensional focusing.

Chip-based microfabricated lenses generally have lower quality than conventional optical elements. Their lack of reconfigurability, poor surface finish, and shape aberration present challenges in the design of optofluidic devices. Here we exploited variations in the physical geometry of the microchannel to form a biconvex fluidic lens in a square expansion chamber, and demonstrated a simple way to manipulate the shape of the lens and its focal distance in real time by using fluidic means without mechanical moving parts. We showed that the use of L^2 technology with a cladding liquid possessing a refractive index matched to the channel material can provide good beam quality. Geometric aberrations of the lens can be corrected by adjusting the shape of the expansion chamber. The loss of light out of the propagation plane due to refraction at the liquid–liquid interfaces is currently limiting the focusing efficiency of our lens, but such losses could be mitigated by waveguiding the light in the plane of the channels.

The quality of the optical interfaces and the range of focal lengths of the L^2 lens are similar to those of tunable microfabricated spherical lenses with tuning mechanisms based on electrowetting,[7,12] changes in the volume of the liquids constituting the lens,[8–10,13–15] and changes in the refractive index of the liquid surrounding the lens.[11] We could not find references on the efficiency and enhancement factor of these spherical lenses; they should, in principle, achieve higher intensity enhancement factors than cylindrical lenses. The spherical lenses demonstrated so far can only focus light perpendicular to the plane of the device, however, and often require more complex fabrication procedures. Our lens focuses light in the plane of the substrate, and is simple to fabricate. The L^2 lens is a promising technology for the development of tunable micro-scale lenses with qualities similar to those of standard optics ready for planar integration for lab-on-a-chip applications.

Along with the L^2 lens, we also developed a convenient technique for beam tracing in a microfluidic system. Despite recent efforts in the development of micro-scale optical elements, there is no simple way for characterization of these elements on a chip. Some of the previous work on microfabricated lenses have characterized light beams by introducing alumina particles in PDMS[5] or fluorescent dye in a narrow channel[3,4,6] to show that the intensity of the focused light increased, but such methods could not identify the focal point of the lens. By placing a large chamber filled with fluorescent dyes in the optical path, we demonstrated that it is possible to trace the beam, identify the focal point, and analyze the beam quality, in a planar optical system that is enclosed in a transparent material (PDMS in this case). This method should be useful for microsystems where conventional beam profilers and related devices that rely on free-space optics are too bulky as an analytical tool.

Acknowledgements

We thank Professor Howard Stone, Dr Eric Mack, Dr Patrick Hung, and Andrew Lee for helpful discussions. This work was supported by the Center for Optofluidic Integration of the Defense Advanced Research Projects Agency.

References

1 V. Lien, K. Zhao, Y. Berdichevsky and Y.-H. Lo, *IEEE J. Sel. Top. Quantum Electron.*, 2005, **11**, 827–834.
2 V. Lien, K. Zhao and Y.-H. Lo, *Appl. Phys. Lett.*, 2005, **87**, 194106/194101–194106/194103.
3 Z. Wang, J. El-Ali, M. Engelund, T. Gotsaed, I. R. Perch-Nielsen, K. B. Mogensen, D. Snakenborg, J. P. Kutter and A. Wolff, *Lab Chip*, 2004, **4**, 372–377.
4 J. Seo and L. P. Lee, *Sens. Actuators, B*, 2004, **B99**, 615–622.
5 J. Godin, V. Lien and Y. -H. Lo, *Appl. Phys. Lett.*, 2006, **89**, 061106/061101–061106/061103.
6 S. Camou, H. Fujita and T. Fujii, *Lab Chip*, 2003, **3**, 40–45.

7 B. Berge and J. Peseux, *Eur. Phys. J. E*, 2000, **3**, 159–163.
8 N. Chronis, G. L. Liu, K.-H. Jeong and L. P. Lee, *Opt. Express*, 2003, **11**, 2370–2378.
9 L. Dong, A. K. Agarwal, D. J. Beebe and H. Jiang, *Nature*, 2006, **442**, 551–554.
10 L. Dong and H. Jiang, *Appl. Phys. Lett.*, 2007, **91**, 041109/041101–041109/041103.
11 K. -S. Hong, J. Wang, A. Sharonov, D. Chandra, J. Aizenberg and S. Yang, *J. Micromech. Microeng.*, 2006, **16**, 1660–1666.
12 S. Kuiper and B. H. W. Hendriks, *Appl. Phys. Lett.*, 2004, **85**, 1128–1130.
13 N. Sugiura and S. Morita, *Appl. Opt.*, 1993, **32**, 4181–4186.
14 A. Werber and H. Zappe, *Appl. Opt.*, 2005, **44**, 3238–3245.
15 D. -Y. Zhang, V. Lien, Y. Berdichevsky, J. Choi and Y.-H. Lo, *Appl. Phys. Lett.*, 2003, **82**, 3171–3172.
16 T. M. Squires and S. R. Quake, *Rev. Mod. Phys.*, 2005, **77**, 977–1026.
17 D. B. Wolfe, R. S. Conroy, P. Garstecki, B. T. Mayers, M. A. Fischbach, K. E. Paul, M. Prentiss and G. M. Whitesides, *Proc. Natl. Acad. Sci. U. S. A.*, 2004, **101**, 12434–12438.
18 J. C. McDonald, D. C. Duffy, J. R. Anderson, D. T. Chiu, H. Wu, O. J. A. Schueller and G. M. Whitesides, *Electrophoresis*, 2000, **21**, 27–40.
19 Commercially available PDMS (Sylgard 184) contains nanoparticles of silica that scatter light. In the devices we fabricated, the thickness of PDMS along the optical path was limited (~2–3 cm), and scattering due to passage of light through PDMS did not cause significant loss.
20 It is possible to use a chamber with higher ratio of width (x_e) to length (y_e) to achieve a larger curvature. The size of recirculation zones, however, increases significantly for a ratio of $x_e : y_e > 1.5$. Increasing the aspect ratio of the chamber does not increase the core-cladding curvature further.
21 H. K. Moffatt, *J. Fluid Mech.*, 1964, **18**, 1–18.
22 S. Taneda, *J. Phys. Soc. Jpn.*, 1979, **46**, 1935–1942.
23 F. Durst, J. C. F. Pereira and C. Tropea, *J. Fluid Mech.*, 1993, **248**, 567–581.
24 T. Hawa and Z. Rusak, *J. Fluid Mech.*, 2001, **436**, 283–320.
25 J. Mizushima, H. Okamoto and H. Yamaguchi, *Phys. Fluids*, 1996, **8**, 2933–2942.
26 J. N. Lee, C. Park and G. M. Whitesides, *Anal. Chem.*, 2003, **75**, 6544–6554.
27 We developed a simple ray tracing program in Matlab which assumes that the shape of the liquid–liquid interface is a circle, and estimated the range of focal distances of the L^2 lens.
28 H. G. Elias, Refractive Indices of Common Solvents, in *Polymer Handbook, Fourth Edition*, ed. J. Brandrup, E. H. Immergut, E. A. Grulke, A. Abe, and D. R. Bloch, Wiley-Interscience, New York, 1999.
29 Commercially available benzothiazole (from Sigma Aldrich) has a brown color due to impurities. We measured the extinction coefficient of neat benzothiazole (9.17 M) to be about 0.07 $M^{-1}cm^{-1}$ at 532 nm using a UV-Visible spectrometer. Benzothiazole filtered with activated carbon had an extinction coefficient of about 0.01 $M^{-1}cm^{-1}$ at 532 nm. When the 1 mm expansion chamber was filled with this filtered benzothiazole, the loss due to absorption was less than 3% of the incident light, and was not the limiting factor in the efficiency and light enhancement ability of the lens.
30 D. B. Wolfe, D. V. Vezenov, B. T. Mayers, G. M. Whitesides, R. S. Conroy and M. G. Prentiss, *Appl. Phys. Lett.*, 2005, **87**, 181105/181101–181105/181103.
31 S. K. Y. Tang, B. T. Mayers, D. V. Vezenov and G. M. Whitesides, *Appl. Phys. Lett.*, 2006, **88**, 061112/061111–061112/061113.
32 R. F. Ismagilov, A. D. Stroock, P. J. A. Kenis, G. Whitesides and H. A. Stone, *Appl. Phys. Lett.*, 2000, **76**, 2376–2378.
33 Simulation from our Matlab ray tracing program.
34 Relaxation time is the characteristic time in which the shape of the lens relaxes to its new shape after a change in flow rate. We assume that the curvature approaches its steady-state value exponentially: $R_{curvature}(t) = R_{curvature}(t = \infty) + \Delta R_{curvature}\ exp(-\frac{t}{\tau})$, where $\Delta R_{curvature} = R_{curvature}(t = \infty) - R_{curvature}(t = 0)$. The relaxation time is the exponential timescale of this process, τ. See also Fig. S2 in ESI†.
35 W. T. Anderson and D. L. Phillen, *J. Lightwave Technol.*, 1983, **LT–1**, 20–26.
36 We only reported focal distance here. It is different from the focal length of the lens, which is the distance at which collimated light will be focused to a single spot.
37 We treated the aperture as an one-dimensional single slit, and defined the diffraction-limited beam width at the focal point as the distance, in the focal plane, between the central maxima and the first minima of the diffracted plane wave.
38 X. Mao, J. R. Waldeisen, B. K. Juluri and T. J. Huang, *Lab Chip*, 2007, **7**, 1303–1308.
39 Y. Yamaguchi, T. Honda, M. P. Briones, K. Yamashita, M. Miyazaki, H. Nakamura and H. Maeda, *Chem. Eng. Technol.*, 2007, **30**, 379–382.
40 Y. Yamaguchi, T. Honda, M. P. Briones, K. Yamashita, M. Miyazaki, H. Nakamura and H. Maeda, *Meas. Sci. Technol.*, 2006, **17**, 3162–3166.
41 S. K. Yoon, M. Mitchell, E. R. Choban and P. J. A. Kenis, *Lab Chip*, 2005, **5**, 1259–1263.
42 Since the beam-tracing chamber was filled with a dye dissolved in ethylene glycol with refractive index 1.012 times higher than that of PDMS, we estimated the measured focal distance here to be 1.012 times longer than the case when the beam propagated in PDMS only using paraxial approximation.